Dalton Transactions

ROYAL SOCIETY OF CHEMISTRY

PAPER

View Article Online
View Journal | View Issue

Cite this: *Dalton Trans.*, 2025, **54**, 328

Water-soluble photocatalysts based on porphyrin-carbon dot conjugates produce H_2 under visible light irradiation†

Katerina Achilleos,‡[a] Anna Katsari,‡[a] Emmanouil Nikoloudakis, *[b] Foteini Chatzipetri,[a] Dimitris Tsikritzis, [c] Kalliopi Ladomenou, *[d] Georgios Charalambidis, *[e] Emmanuel Stratakis [b,f] and Athanassios G. Coutsolelos *[a,b]

Received 22nd July 2024,
Accepted 1st November 2024

DOI: 10.1039/d4dt02101k

rsc.li/dalton

Herein, we report visible-light-induced hydrogen generation from aqueous protons utilizing a novel hybrid photocatalytic nanomaterial comprising porphyrin-carbon dot conjugates. Amide coupling between metallated tetra-carboxyphenyl porphyrins (MTCPPs) and nitrogen doped carbon dots (**NCDots**) was performed to afford M-TCPP-NCDots hybrids, which were applied in hydrogen evolution photocatalysis under visible irradiation. H_2 was obtained in the presence of appropriate sacrificial electron donors and with no additional metallic co-catalysts. It is noteworthy that the covalent attachment as well as the zinc-metallation of the porphyrin moiety were proved vital for the efficiency of the present system. The present study constitutes an innovative approach for artificial photosynthesis avoiding the use of costly materials such as noble metals.

Introduction

The escalating demand for energy along with the environmental challenges resulting from the overexploitation of fossil fuels makes the exploitation of renewable energy sources imperative.[1] Among these, solar energy stands out as the most promising alternative since it is abundant and environmentally friendly. Efficient and low-cost photocatalytic hydrogen production from water is a major focus of research toward solar energy conversion and storage.[2] H_2 is considered as a prospective fossil-fuel alternative due to its high energy density and the absence of harmful emissions, since the only product from its combustion is H_2O.[3] The use of hydrogen as an alternative fuel represents a longstanding strategy for globally reducing carbon dioxide emissions.[4] Conventional approaches of hydrogen generation, like steam reforming of fossil fuels or electrolysis of water, involve substantial energy losses, resulting in low efficiency.[5] Therefore, solar driven H_2 evolution is the most appealing approach.[6] In the pursuit of sustainable energy solutions, the exploration of novel molecules and materials for the development of efficient photocatalytic systems has become paramount. Among these materials, carbon dots (CDs), nitrogen-doped carbon dots (**NCDots**) and porphyrins have emerged as intriguing components in light-driven hydrogen production schemes.[7] Most photocatalytic systems consist of three essential components: the photosensitizer (PS), the catalyst and the sacrificial electron donor (SED). Porphyrin derivatives have been employed in several artificial photosynthetic systems due to their easily modifiable structure, various interaction mechanisms with materials, and high molar absorption coefficient in the visible region.[8] Owing to their efficient energy and/or charge-transfer capabilities, they are primarily used as PSs in various photocatalytic schemes.[9,10] Moreover, porphyrins have also been employed as catalysts for the hydrogen evolution reaction (HER), as their aromatic macrocycle greatly enriches the redox chemistry of metal centers providing improved catalytic performance.[11,12]

Carbon dots and nitrogen-doped carbon dots represent a promising new class of low-cost carbon nanomaterials, gathering significant attention due to their unique optical, elec-

[a]*Laboratory of Bioinorganic Chemistry, Chemistry Department, University of Crete, 70013 Heraklion, Crete, Greece. E-mail: acoutsol@uoc.gr*
[b]*Foundation for Research and Technology (FORTH), Institute of Electronic Structure and Laser (IESL), 70013 Heraklion, Greece. E-mail: enikoloudakis@iesl.forth.gr*
[c]*Department of Electrical & Computer Engineering, Hellenic Mediterranean University (HMU) Heraklion, Crete 71410, Greece*
[d]*Hephaestus Laboratory, School of Chemistry, Faculty of Sciences, Democritus University of Thrace, Kavala, Greece. E-mail: kladomenou@chem.duth.gr*
[e]*Theoretical and Physical Chemistry Institute, National Hellenic Research Foundation, 48 Vassileos Constantinou Ave., 11635 Athens, Greece. E-mail: gcharal@eie.gr*
[f]*Qingdao Innovation and Development Center, Harbin Engineering University, Qingdao 266000, Shandong, P. R. China*

†Electronic supplementary information (ESI) available. See DOI: https://doi.org/10.1039/d4dt02101k

‡These two authors contributed equally to this work.

tronic, and surface area properties.[13] CDs have recently been functionalized with porphyrin dyes either *via* non-covalent supramolecular interactions[14,15] or through direct covalent linkages, resulting in the formation of hybrid nanomaterials with interesting properties.[16,17] Furthermore, CDs can undergo charge-transfer reactions, acting as either electron donors or acceptors in their excited state. Based on this, CDs have shown great potential as PSs in photocatalytic H_2 generation, in the presence of molecular catalysts.[18–20] Additionally, CDs have been combined with several nanomaterials, such as CdS nanoparticles, acting as electron acceptors and suppressing photo-excited carrier recombination during light driven H_2 formation.[21] Notably, Guldi and co-workers prepared novel CDs with dual functionality, operating as photocatalysts.[7] These CDs absorb light and produce H_2 from water, without the need for an external PS or catalyst.

In this report, we covalently connected *tetra*-carboxy-substituted porphyrin derivatives (as a free base or metalated with Zn) to **NCDots** and the resulting hybrid nanomaterials (Scheme 1) were investigated for light induced H_2 evolution. The present noble metal free photocatalysts demonstrated high activity in H_2 production without the need for additional metallic co-catalysts and remained stable for several days under continuous light irradiation. It is important to note that this is the first example of **NCDots** operating as catalysts, in combination with a molecular PS in H_2 evolving systems.

Results and discussion

Synthesis and characterisation

The porphyrin-NCDots conjugates were synthesized *via* amide coupling between carboxy-porphyrin derivatives (MTCPPs) and nitrogen-doped carbon dots (Scheme 1). Porphyrin precursor molecules **TCPP** and **ZnTCPP** were prepared according to published procedures.[22] **NCDots** were synthesized according to a simple bottom-up method using citric acid and ethylenediamine as carbon and nitrogen sources, respectively.[18] The corresponding **NCDots** possess a variety of oxygen and nitrogen functional groups and in particular the presence of the amino groups enables their linkage with the carboxy-porphyrins. The final hybrid materials were fully characterized by NMR, XPS, IR, UV-Vis and fluorescence spectroscopy techniques as well as SEM. The successful covalent functionalization of the **NCDots** surface with porphyrins was verified initially by ^{1}H NMR spectroscopy (Fig. S1–S5†). The porphyrin-based resonances were all present in the spectra of the hybrids (**TCPP-NCDots** and **ZnTCPP-NCDots**), along with signals expected for **NCDots**. Remarkably, in both hybrids (at around 10 ppm) we observed a signal that corresponds to the amide proton with an integration close to 1 in relation to the porphyrin β-pyrrolic peaks (integral equals 8). This proves the successful amide coupling and suggests that only 1 of the 4 carboxylic peripheral moieties of each porphyrin molecule is used for the coupling. Additional evidence for the successful covalent formation of hybrids was obtained from the Kaiser test (see the ESI for details†).[23,24] From these measurements, we calculated the number of free (non-reacted) amino groups in **TCPP-NCDots** and **ZnTCPP-NCDots** (Fig. S6a–f and Table S1†) and in both cases a similar degree of functionalization (~90%) was achieved. Scanning electron microscopy studies were performed to investigate the size and the morphology of the synthesized porphyrin-NCDots conjugates. As illustrated in Fig. 1, both **TCPP-NCDots** and **ZnTCPP-NCDots** hybrids aggregate into poorly formed spherical architectures with a diameter of ~190 nm. This radius is increased compared to pristine **NCDots** (Fig. S6g†) and previous reports concerning similar materials.[18]

Spectroscopic characterization (FT-IR and UV-visible)

FT-IR spectroscopy was performed to obtain further information about the surface functionalization of **TCPP-NCDots** and **ZnTCPP-NCDots** conjugate materials (Fig. S7†). In Fig. S7a,† the spectra of all compounds containing **NCDots** are presented. The broad bands at 3670–3160 cm^{-1} correspond to N–H and O–H vibrations, while the peak at 2940 cm^{-1} is attributed to C–H stretching. This is in accordance with previous reports on CDots prepared using citric acid as a carbon source.[25,26] The absorption bands in the range of 1730–1630 cm^{-1} are attributed to the asymmetric stretching vibration of C=O groups and the peak at 1533 cm^{-1} originates from the N–H bending vibration. Based on the above observations, we conclude that the hybrid materials retain their characteristic **NCDots**-based features. Fig. S7b† highlights

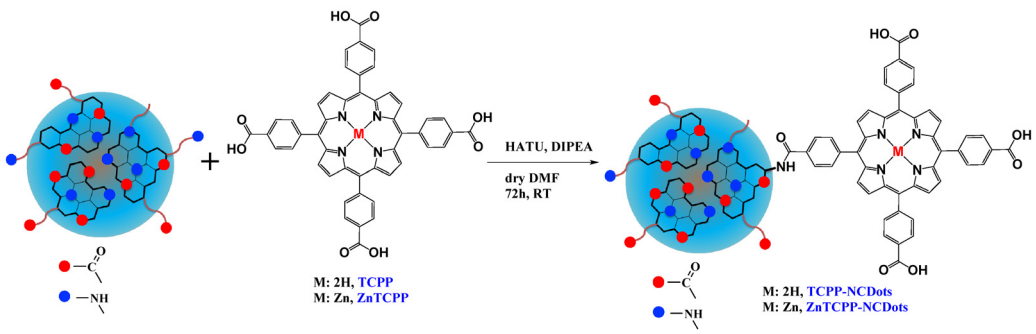

Scheme 1 Synthetic procedure for the synthesis of **TCPP-NCDots** and **ZnTCPP-NCDots** photocatalysts.

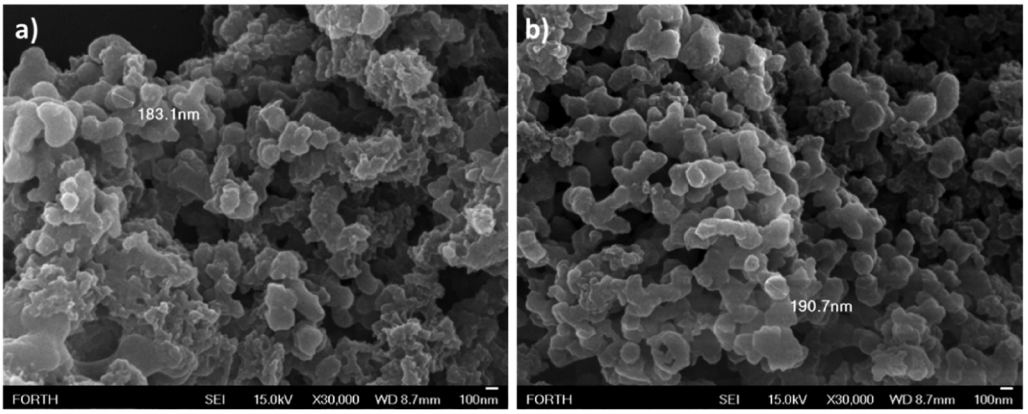

Fig. 1 Scanning electron microscopy images of (a) **TCPP-NCDots** and (b) **ZnTCPP-NCDots**, from aqueous solution after drop-casting onto a glass substrate.

specific peaks to facilitate the comparison of vibrational peaks between precursor porphyrin molecules and porphyrin-**NCDots**. The intense peak at 1683 cm^{-1} in both **TCPP** and **ZnTCPP** corresponds to C═O stretching and is also dominant in the **TCPP-NCDots** and **ZnTCPP-NCDots** spectra, while the feature at 1636 cm^{-1} (C═O stretching) is mainly derived from the **NCDots** moiety. The peak at 1599 cm^{-1} is attributed to C═C/C═N stretches and is present in both the precursor porphyrins and the hybrid materials, but is absent in the non-functionalized **NCDots**. The signals in the range of 1425–1340 cm^{-1} are attributed to the sp^3 C–H bending and symmetric stretching vibration of the carboxylate groups.[27] Additionally, the evolution of new features in the range of 1230–1140 cm^{-1} in the spectra of both hybrids can be assigned to the O–H vibration of the carboxylate groups from the porphyrin moiety.

The UV-Vis absorption spectra of the synthesized conjugates demonstrated all characteristic peaks of the **NCDots** and porphyrin components (Fig. 2). In detail, the pristine **NCDots** presented an absorption band at 340 nm, which is attributed to the n → π* transition of the C═O bond.[28] The absorption spectrum of the free base **TCPP** revealed the typical Soret-band at 416 nm and four Q-band absorptions at 512, 546, 590 and 646 nm. Similarly, the spectrum of the metalated **ZnTCPP** derivative exhibited the Soret band at 425 nm and two Q bands at 556 and 597 nm. The free base conjugate, **TCPP-NCDots**, displayed the broad peak of **NCDots** at 348 nm (red-shifted by 8 nm), along with the typical Soret band at 416 nm and Q bands at 512, 545, 589 and 646 nm, attributed to the porphyrin ring. In the case of the zinc metalated hybrid **ZnTCPP-NCDots**, the carbon-dot-based absorption band was observed at 346 nm, which is red-shifted by 6 nm compared to the pristine **NCDots**. In addition, the Soret and Q-band absorptions were also red-shifted to 430 nm and 561 and 601 nm, respectively. The observed red shift of the porphyrin absorption maxima could be attributed either to the close proximity between **NCDots** and **ZnTCPP** and their electronic communication in the ground state or to the formation of *J*-aggregates (side by side) of the porphyrin macrocycle moieties on the surface of the nanomaterial.[29]

Fluorescence and X-ray photoelectron spectroscopy studies

Fluorescence studies revealed that the emission of **NCDots** depends strongly on the excitation wavelength, as shown in Fig. 3a. This excitation–dependent behaviour is a well-known feature of carbon dot materials.[30,31] In the pristine **NCDots**,

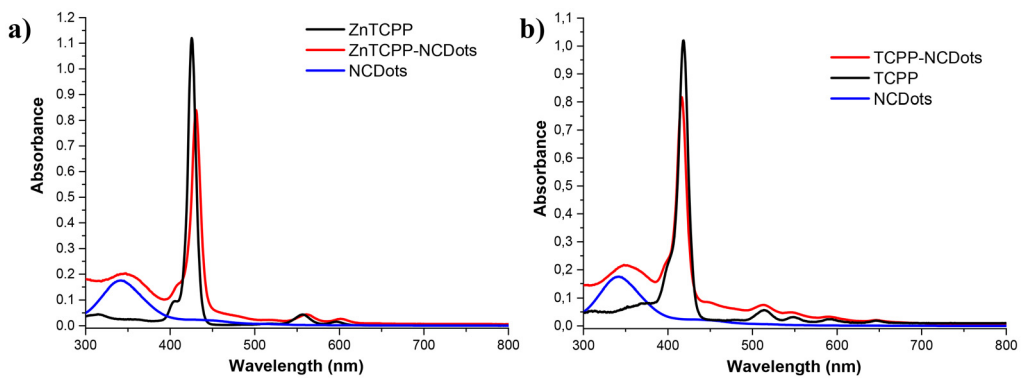

Fig. 2 UV-Vis absorption spectra in DMSO of (a) **NCDots**, **ZnTCPP** and **ZnTCPP-NCDots** and (b) **NCDots**, **TCPP** and **TCPP-NCDots**.

the emission maximum was observed at 443 nm after excitation at 340 nm. The fluorescence spectra of the two hybrids **TCPP-NCDots** and **ZnTCPP-NCDots** displayed the characteristic wavelength-dependent **NCDots**-based emission, along with the porphyrin fluorescence bands at 651 nm and 715 nm for the free base material and 607 nm and 656 nm for the zinc derivative (Fig. 3b and c). Interestingly, the red shift of the **NCDots**-based emission maxima as we alter the excitation wavelength from 300 nm to 480 nm is more intense in the case of the two conjugates (111 nm and 120 nm) compared to the pristine **NCDots** (95 nm) (Fig. S8†). This observation indicates that the covalent coupling affects significantly the photophysical characteristics of the nanomaterial. On the other hand, the porphyrin-based emission is not excitation-dependent, as expected.

We proceeded to analyze the samples with X-ray photoelectron spectroscopy (XPS). Fig. S9† shows the C 1s peak of all the samples. The spectra were charge-referenced by setting the C–C peak at 248.8 eV. Upon initial examination, we observed a distinct difference in the peak shape between the **NCDots** and the porphyrins. The C 1s peak of the porphyrins exhibited a highly asymmetric profile, featuring a prominent peak corresponding to C–C bonds, as well as secondary features at higher binding energies attributed to carbon in functional groups containing oxygen and nitrogen. In contrast, the C 1s peak of the **NCDots** displayed a wider, asymmetric shape, suggesting a greater presence of carbon bonded to oxygen and nitrogen species. To further analyze the XPS data, we fitted the experimental points using peaks assigned to C–C, C–O/C–N, –C═O, –COO, and π–π* transitions at 284.8 eV, 286.4 eV, 288.1 eV, 289.2 and 291.4 eV, respectively. To quantitatively assess the atomic percentage concentration of carbon species, we compiled the fitting results in Table S2.† The C 1s spectra and atomic percentage of carbon–oxygen species for **TCPP** and **ZnTCPP** were consistent with expectations and aligned with the existing literature. It is important to note that adventitious carbon was present on the sample surfaces, contributing to a small extent to the C 1s and O 1s signals. Table S2† also reveals a high content of oxygen bonded to carbon in the **NCDots**, reaching up to 50%,[32] while the porphyrin samples exhibited a high concentration of C–C content. The C–C content increases for the **ZnTCPP-NCDots** and **TCPP-NCDots**, which indicates the functionalization of **NCDots** by the porphyrins. Fig. S10† presents the N 1s spectra for all samples. In most spectra, a weak peak originating from the Mo $3p_{3/2}$ band of the Mo holder was observed at approximately 395 eV. The N 1s peak of the **NCDots** displayed a wide, symmetric shape, possibly attributed to different chemical states of N atoms that could not be resolved in our current XPS resolution. Conversely, the N 1s spectrum of **TCPP** exhibited the typical shape of porphyrins, with two resolved peaks representing different chemical environments of the N atoms in the porphyrin core. The lower binding energy peak at 398.2 eV was assigned to iminic (–N═) nitrogen, while the higher binding

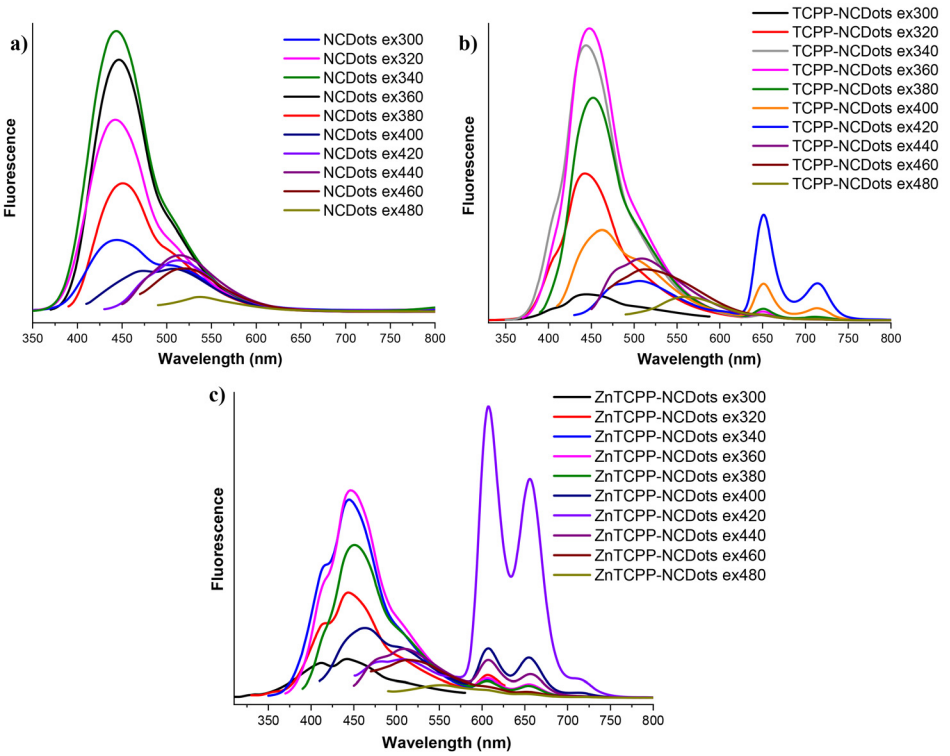

Fig. 3 Fluorescence emission spectra in DMSO of (a) **NCDots**, (b) **TCPP-NCDots** and (c) **ZnTCPP-NCDots**.

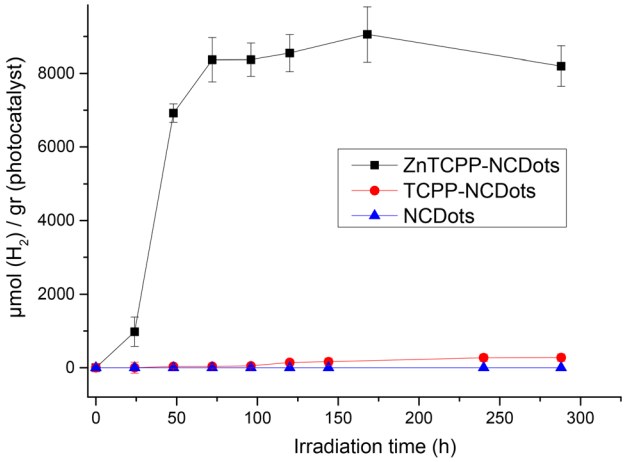

Fig. 4 Photocatalytic hydrogen production plots of **ZnTCPP-NCDots** (black line), **TCPP-NCDots** (red line) and **NCDots** (blue line). The presented results are the average values of three independent measurements (within 10% error).

energy peak at 400.1 eV corresponded to pyrrolic (–NH) nitrogen.[33,34] Notably, the N 1s peaks of the **TCPP-NCDots** and **ZnTCPP-NCDots** did not show any significant changes in the position of the peak and spectral shape compared to the N 1s peak of the **NCDots**, suggesting the presence of a thin film of porphyrins on the surface of the functionalized **NCDots**. Table S3† reports the binding energies of the N 1s peak for all the samples and of the Zn $2p_{3/2}$ peak. The N 1s of **ZnTCPP** is located at 398.6 eV in excellent agreement with similar Zn porphyrins.[35] Fig. S11† displays the characteristic peaks of the metal in the porphyrin core. The peaks observed in the **ZnTCPP-NCDots** samples exhibit significantly lower intensity. The Zn $2p_{3/2}$ peak of **ZnTCPP** is located at 1022.2 eV, indicating the Zn^{2+} oxidation state.[35,36]

Photocatalytic hydrogen generation studies

Photocatalytic experiments were performed under visible light irradiation using 5 mg of each nanomaterial as a photocatalyst in aqueous solution with the use of diverse sacrificial electron donors (SEDs), namely tris(carboxyethyl)-phosphine/ascorbic acid (TCEP/Asc). The concentration of the TCEP/Asc 1 : 1 solution was 0.1 M and the pH was adjusted to 5. This SED mixture has previously presented enhanced catalytic efficiency towards H_2 evolution, since TCEP regenerates oxidized ascorbic acid, thereby overcoming the instability of Asc and extending the lifetime of the system.[18,19,37,38] Photocatalytic studies demonstrated that both porphyrin-**NCDots** conjugate nanomaterials are able to produce H_2. On the other hand, **NCDots** alone as well as control experiments lacking the photocatalyst, or the SED, or light irradiation, displayed no H_2 production. Moreover, the non-covalent combination (physical mixture) of either **ZnTCPP** or **TCPP** with **NCDots** did not

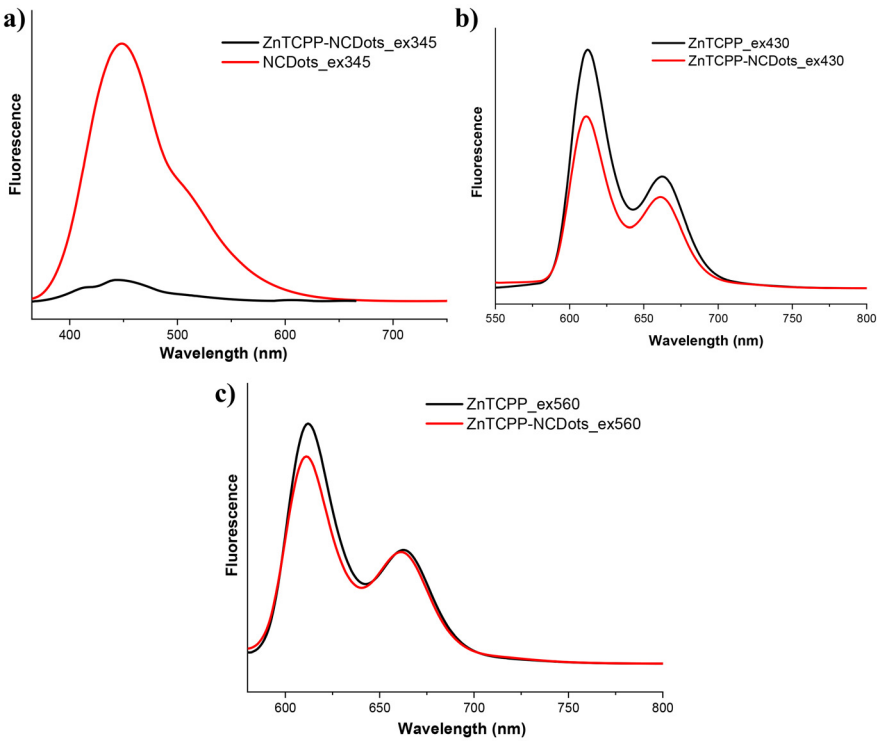

Fig. 5 Fluorescence emission spectra in DMSO solutions of (a) **ZnTCPP-NCDots** and **NCDots** upon excitation at 345 nm, (b) **ZnTCPP-NCDots** (concentration = 0.003 mg mL^{-1}) and **ZnTCPP** (concentration = 0.26 × 10^{-6} M) upon excitation at 430 nm and (c) **ZnTCPP-NCDots** (concentration = 0.003 mg mL^{-1}) and **ZnTCPP** (concentration = 0.26 × 10^{-6} M) upon excitation at 560 nm.

present any H_2 generation probably due to the insolubility of the porphyrin molecules in the acidic aqueous buffer solution. The later observation demonstrates the necessity of the covalent attachment to achieve photocatalytic H_2 production in the present system. Upon optimization of the system, **ZnTCPP-NCDots** exhibited a maximum catalytic activity of 9 ± 1 mmol g^{-1} after 168 h of irradiation but had already reached 8.3 mmol g^{-1} after 72 h of irradiation (with a rate of 0.115 ± 0.02 mmol g^{-1} h^{-1}) (Fig. 4). It is noteworthy that the free base conjugate presented negligible H_2 evolution (0.2 ± 0.02 mmol g^{-1}) compared to the Zn metalated nanomaterial.

As demonstrated in Fig. 4, H_2 evolution reaches a plateau after several hours of irradiation. The addition of SED does not regenerate the catalytic system but when the photocatalyst (**ZnTCPP-NCDots**) was added, the catalytic activity was effectively restored. This observation suggests that the porphyrin-**NCDots** nanomaterial decomposed after about 3 days of visible light irradiation. This observation was further supported by UV-Vis spectroscopy measurements, which showed that all porphyrin-based peaks had vanished after the catalysis (Fig. S12 and S13†).

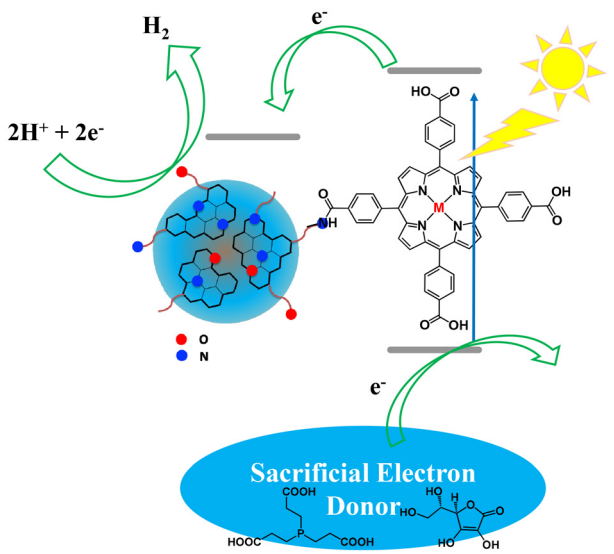

Fig. 6 Proposed mechanism for H_2 generation.

In order to shed light on the catalytic mechanism of this system, we investigated the excited state of **ZnTCPP-NCDots** by selectively exciting the **NCDots** and the porphyrin constituents and comparing them with the **NCDots** and **ZnTCPP** references after adjusting to the same optical density (A = 0.1). Upon selective excitation of the **NCDots** moiety at 345 nm, a quantitative quenching of the **NCDots** fluorescence at 448 nm was observed in the **ZnTCPP-NCDots** hybrid (Fig. 5a), indicating a strong electronic interaction between the two components. In addition, when the porphyrin chromophore was selectively excited at 430 nm (S2 excited state), a significant fluorescence quenching was observed in the **ZnTCPP-NCDots** hybrid (Fig. 5b), possibly due to an electron transfer process from the **ZnTCPP** to the **NCDots**. Surprisingly, when the zinc porphyrin was selectively excited at 560 nm (S1 excited state), no significant quenching was revealed between **ZnTCPP** and **ZnTCPP-NCDots** (Fig. 5c). These findings are in strong agreement with the work of Arcudi *et al.*,[39] who verified that the charge separated states of the porphyrin-**NCDots** conjugates are above the S1 and below the S2 porphyrin singlet excited states. Thus, the electron transfer from the zinc porphyrin to **NCDots** is possible only after excitation of the porphyrin to the S2 excited state. Lifetime decay fluorescence measurements (Fig. S14†) were also performed to study the electronic interactions of the two components in the **ZnTCPP-NCDots** hybrid. The pristine **NCDots** presented two lifetimes, τ_1 = 3.7 ns (38%) and τ_2 = 14.7 ns (62%). These values were calculated by using a double-exponential function for satisfactory data fitting. These measurements are consistent with the literature,[40,41] since it is known that carbon dot materials show multiexponential decay of photoluminescence emission. **ZnTCPP** showed a mono-exponential decay with τ_1 = 2.2 (100%) ns, which is a regular value for zinc metalated porphyrins. Interestingly, **ZnTCPP-NCDots** exhibited double-exponential decay with τ_1 = 0.9 (28%) ns and τ_2 = 5.1 (72%) ns. The short one (0.9 ns) is porphyrin based and is significantly quenched compared to the **ZnTCPP**. This finding further supports the strong electronic communication between **ZnTCPP** and **NCDots** in the excited state. Based on the above results, we propose that during the photocatalytic H_2 evolution, after light excitation of the porphyrin moiety to the S2 excited state, electrons are injected towards the NCDot-moiety and aqueous protons are reduced to H_2, while the SED mixture regenerates the oxidized photocatalyst (Fig. 6).

Table 1 Comparison between the best carbon-dot-based systems in the literature and this work

Photocatalyst	SED	H_2 production	Ref.
ZnTCPP-NCDots	TCEP/Asc	0.115 mmol g^{-1} h^{-1}	This work
CQD-NiP	EDTA	0.398 mmol g^{-1} h^{-1}	20
CQD/TiO_2	TEOA	0.472 mmol g^{-1} h^{-1}	42
CQD/TiO_2/Pt	TEOA	1.458 mmol g^{-1} h^{-1}	42
Au/CQDs	H_2O/MeOH	0.250 mmol g^{-1} h^{-1}	43
Amino-conjugated CQDs	Na_2S/Na_2SO_3	0.273 mmol g^{-1} h^{-1}	44
$[ZnTMPyP]^{4+}$/MoS_2/RGO	TEOA	2.56 mmol g^{-1} h^{-1}	45

Conclusions

In summary, we synthesized porphyrin and nitrogen-doped carbon dot conjugates, covalently connected *via* amide coupling and investigated their photocatalytic ability for visible light driven H_2 evolution ability in aqueous media. A mixture of TCEP and Asc was used as the sacrificial reagent, enabling prolonged H_2 production. Importantly, the covalent connection between the porphyrin and **NCDots** was shown to be essential for efficient light driven H_2 generation in this system. The **ZnTCPP-NCDots** photocatalyst, which demonstrated considerable stability, achieved an H_2 production of 9 mmol g^{-1} after 168 h of visible light irradiation without the need for any additional co-catalyst. The highest production rate was 0.115 mmol·g^{-1}·h^{-1}, which, while modest, is comparable to the values reported in the literature for this type of material (Table 1). This work highlights the great potential of carbon-based nanomaterials combined with noble metal-free porphyrin dyes as efficient water-soluble photocatalysts for the HER.

Experimental

Materials

All reagents were purchased from common commercial sources and used without any further purification, unless otherwise stated.

Nuclear magnetic resonance (NMR) spectroscopy

The porphyrin moieties were analyzed with ^{1}H NMR spectroscopy using Bruker AMX-500 MHz and Bruker DPX-300 MHz spectrometers. All measurements were carried out at room temperature in a deuterated solvent using residual protons as an internal reference.

Ultraviolet-visible (UV-Vis) absorption spectroscopy

In all studies, a Shimadzu UV-1700 spectrometer was used. The reported experiments were performed using quartz cuvettes with a 0.2 cm path length.

Fluorescence emission spectroscopy

The emission spectra were recorded on a JASCO FP-6500 fluorescence spectrophotometer equipped with a red-sensitive WRE-343 photomultiplier tube (wavelength range: 200–850 nm).

Emission lifetime measurements

The emission lifetimes were determined by the time-correlated single-photon counting (TCSPC) technique using an Edinburgh Instruments mini-tau lifetime spectrophotometer equipped with an EPL 405 pulsed diode laser at 406.0 nm with a pulse width of 71.52 ps and a high-speed red-sensitive photomultiplier tube (H5773-04) as the detector.

X-ray photoelectron spectroscopy (XPS)

The XPS measurements were performed using a SPECS system equipped with a Phoibos 100 1D-DLD hemispherical energy analyzer. A nonmonochromatic Alkα X-Ray line was used to acquire the spectra. The pass energy was set at 30eV, and an electron flood gun was employed for charge compensation during the measurements.

Synthesis

Porphyrin precursor molecules **TCPP** and **ZnTCPP** were synthesized according to published experimental procedures.[22]

Synthesis of TCPP-NCDots. 5,10,15,20-Tetrakis-(4-(carboxy)-phenyl)-porphyrin (TCPP, 0.06 g, 0.076 mmol) was dissolved in dry DMF (6 mL) in a two-necked round-bottomed flask under a nitrogen atmosphere at room temperature. Then, 1-[Bis(dimethylamino)methylene]-1*H*-1,2,3-triazolo[4,5-*b*]pyridinium 3-oxide hexafluorophosphate (HATU, 0.12 g, 0.318 mmol) was added and after stirring for 5 minutes, *N*,*N*-diisopropylethylamine (DIPEA, 0.12 mL, 0.72 mmol) was introduced into the reaction mixture. At the same time, **NCDots** (0.12 g) were added to a Schlenk tube and dissolved in dry DMF (6 mL) and left for stirring, until they were fully dissolved. Then, the **NCDots** solution was added to the two-necked round-bottomed flask with the porphyrin solution and stirred under a nitrogen atmosphere for 72 hours. Then, the solvent was distilled under vacuum and the residue was centrifuged with an ethanol and water solution (1 : 1). The supernatant was collected, and the product was obtained after the distillation of the solvents. Recrystallization with ethanol–petroleum ether afforded the desired hybrid as a brown solid (0.1 g).

UV-Vis λ_{max}, nm 350, 416, 512, 545, 589, 646.

Synthesis of ZnTCPP-NCDots. [(5,10,15,20-Tetrakis-(4-(carboxy)-phenyl))-porphyrinato]-Zn (0.063 g, 0.07 mmol) was dissolved in dry DMF (6 mL) in a two-necked round-bottomed flask under a nitrogen atmosphere at room temperature. Then, HATU (0.12 g, 0.318 mmol) was added and after stirring for 5 minutes, DIPEA (0.12 mL, 0.72 mmol) was introduced into the reaction mixture. At the same time, **NCDots** (0.12 g) were added to a Schlenk tube and were dissolved in dry DMF (6 mL) and were left stirring, until they were fully dissolved. Then, the **NCDots** solution was added to the two-necked round-bottomed flask and stirred under a nitrogen atmosphere for 72 hours, and then the solvent was distilled. Then, the residue was centrifuged with an ethanol and water solution (1 : 1). The product that was present in the supernatant was collected and after the distillation of the solvents, it was recrystallized with ethanol and petroleum ether, dried and isolated as a brown solid (0.108 g).

UV-Vis λ_{max}, nm 346, 430, 561, 602.

Quantitative Kaiser test protocol

The Kaiser test is a sensitive method for the qualitative and quantitative detection of free primary amino groups in non-functionalized **NCDots** along with the free-base and Zn-metalated hybrids (**TCPP-NCDots** and **ZnTCPP-NCDots**).[24,46] The

detection of primary free amino groups is based on their reaction with ninhydrin, which gives an intense blue colour to the solution with an absorption band at 570 nm.[47] When the coupling between **NCDots** and porphyrins is successful, the colour of the solution remains light yellow and there is no significant change. This happens because the reaction between ninhydrin and secondary amines cannot take place.

The procedure involves the preparation of 3 solutions:

1. Solution 1: 10 g of phenol is dissolved in 20 mL of absolute ethanol.

2. Solution 2: 2 mL of KCN aqueous solution (1 mM) is added to 98 mL of pyridine.

3. Solution 3: 1 g of ninhydrin is dissolved in 20 mL of absolute ethanol.

Initially, 200 μg of **NCDots**, **TCPP-NCDots** and **ZnTCPP-NCDots** were added to three separate vials. Afterwards, 75 μL of solution 1, 100 μL of solution 2 and 75 μL of solution 3 were added to each vial. Then, each vial was heated in an oil bath at 120 °C for 5 minutes. Furthermore, 4.75 mL of ultrapure ethanol was added to each vial and as a result the final volume of each one was 5 mL. Finally, the UV-Vis spectrum of the supernatant from each one was recorded, with absorption at 570 nm related to the free primary amino groups.

The result is expressed in μmol of amino groups per g of material as follows:

$$\mathrm{NH_2\ (\mu mol\,g^{-1})} = \frac{[\mathrm{Abs_{sample}} - \mathrm{Abs_{blank}}] \cdot \mathrm{dilution\ (ml)} \times 10^6}{\mathrm{extinction\ coefficient} \cdot \mathrm{sample\ weight\ (mg)}}$$

where dilution is 5 mL, the extinction coefficient is 15 000 M^{-1} cm^{-1} and Abs_{blank} is the absorbance of the corresponding sample without ninhydrin.

Photocatalytic measurements

The photocatalytic H_2 evolution studies were performed in glass vials (14 mL) sealed with a rubber septum, at ambient temperature and pressure. Before each experiment, a fresh buffer solution was prepared. More precisely, the buffer solution was a 0.1 M aqueous solution of tris(carboxyethyl)-phosphine/ascorbic acid (TCEP/Asc) in a 1 : 1 ratio and the pH was regulated to 5. The porphyrin-**NCDots** nanomaterial (5 mg) was added to a glass vial together with 3 mL of the buffer solution. In order to achieve anaerobic conditions, the suspensions were degassed using nitrogen for 5 min (in an ice/water bath). Finally, the samples were sealed with a silicon septum and were irradiated under continuous stirring with a low power white LED lamp ring of 40 W with a colour temperature of 6400 K and a lumen of 3800 LM (Fig. S15†). This set-up provided defined positions and a certain amount (50 W cm^{-2}) of emitted light for all the vials simultaneously (Fig. S16†).

The amount of H_2 produced in each sample vial was determined using a Shimadzu GC 2010 Plus chromatograph with a TCD detector and a molecular sieve 5 Å column (30 m–0.53 mm). For every measurement, 100 μL were taken from the headspace of the vial and were instantly injected into the GC. In all cases, the reported H_2 production values are the averages of three independent experiments.

Calculation of H_2 evolution μmol (H_2) g^{-1} h^{-1}

In every photocatalytic experiment, 0.005 g of porphyrin-NCDots photocatalyst were used. The H_2 evolution was calculated according to the following equation:

$$\mathrm{H_2\ evolution\ \mu mol\ (H_2)\ g^{-1}\ h^{-1}} = \frac{n(\mathrm{H_2})}{m(\mathrm{photocatalyst}) \times t}$$

where $n(H_2)$ is the total amount of the produced H_2 (in μmol), m(photocatalyst) is 0.005 g, and t is the irradiation time in hours (t = 24 h).

Data availability

The data supporting this article have been included as part of the ESI.†

Conflicts of interest

There are no conflicts to declare.

Acknowledgements

This research has been co-financed by the European Union and Greek national funds through the Regional Operational Program "Crete 2014–2020", project code OPS:5029187. Moreover, the European Union's Horizon Europe research and innovation programme under Grant Agreement No. 101119286 (Project: GIANCE) and the Special Research Account of the University of Crete are gratefully acknowledged for the financial support. E. N. gratefully acknowledges the Bodossaki Foundation for its financial support.

References

1 M. S. Reza, N. B. H. Ahmad, S. Afroze, J. Taweekun, M. Sharifpur and A. K. Azad, *Chem. Eng. Technol.*, 2022, **46**, 420–434.

2 U. M. Dankawu, H. Y. Hafeez, C. E. Ndikilar, J. Mohammed, A. B. Suleiman and A. S. Shuaibu, *Int. J. Hydrogen Energy*, 2024, **67**, 1218–1242.

3 A. Le Goff, V. Artero, B. Jousselme, P. D. Tran, N. Guillet, R. Métayé, A. Fihri, S. Palacin and M. Fontecave, *Science*, 2009, **326**, 1384–1387.

4 S. Cao and J. Yu, *J. Photochem. Photobiol., C*, 2016, **27**, 72–99.

5 M. Aravindan and G. P. Kumar, *Results Eng.*, 2023, **20**, 101456.

6 H. Song, S. Luo, H. Huang, B. Deng and J. Ye, *ACS Energy Lett.*, 2022, **7**, 1043–1065.

7 B. Jana, Y. Reva, T. Scharl, V. Strauss, A. Cadranel and D. M. Guldi, *J. Am. Chem. Soc.*, 2021, **143**, 20122–20132.
8 A. Charisiadis, E. Glymenaki, A. Planchat, S. Margiola, A.-C. Lavergne-Bril, E. Nikoloudakis, V. Nikolaou, G. Charalambidis, A. G. Coutsolelos and F. Odobel, *Dyes Pigm.*, 2021, **185**, 108908.
9 E. Nikoloudakis, I. López-Duarte, G. Charalambidis, K. Ladomenou, M. Ince and A. G. Coutsolelos, *Chem. Soc. Rev.*, 2022, **51**, 6965–7045.
10 K. Ladomenou, M. Natali, E. Iengo, G. Charalampidis, F. Scandola and A. G. Coutsolelos, *Coord. Chem. Rev.*, 2015, **304**, 38–54.
11 W. Zhang, W. Lai and R. Cao, *Chem. Rev.*, 2017, **117**, 3717–3797.
12 B. B. Beyene and C.-H. Hung, *Coord. Chem. Rev.*, 2020, **410**, 213234.
13 J. Liu, R. Li and B. Yang, *ACS Cent. Sci.*, 2020, **6**, 2179–2195.
14 V. Villari, M. Gaeta, A. D'Urso and N. Micali, *Colloids Surf., A*, 2022, **648**, 129436.
15 A. Cadranel, V. Strauss, J. T. Margraf, K. A. Winterfeld, C. Vogl, L. Đorđević, F. Arcudi, H. Hoelzel, N. Jux, M. Prato and D. M. Guldi, *J. Am. Chem. Soc.*, 2018, **140**, 904–907.
16 J. R. A. Cosme, H. E. Bryant and F. Claeyssens, *PLoS One*, 2019, **14**, e0220210.
17 C. I. M. Santos, L. Rodríguez-Pérez, G. Gonçalves, S. N. Pinto, M. Melle-Franco, P. A. A. P. Marques, M. A. F. Faustino, M.Á Herranz, N. Martin, M. G. P. M. S. Neves, J. M. G. Martinho and E. M. S. Maçôas, *Carbon*, 2020, **166**, 164–174.
18 K. Ladomenou, G. Landrou, G. Charalambidis, E. Nikoloudakis and A. G. Coutsolelos, *Sustainable Energy Fuels*, 2021, **5**, 449–458.
19 K. Ladomenou, M. Papadakis, G. Landrou, M. Giorgi, C. Drivas, S. Kennou, R. Hardré, J. Massin, A. G. Coutsolelos and M. Orio, *Eur. J. Inorg. Chem.*, 2021, **2021**, 3097–3103.
20 B. C. M. Martindale, G. A. M. Hutton, C. A. Caputo and E. Reisner, *J. Am. Chem. Soc.*, 2015, **137**, 6018–6025.
21 Y. Yu, Q. Zeng, S. Tao, C. Xia, C. Liu, P. Liu and B. Yang, *Adv. Sci.*, 2023, **10**, 2207621.
22 V. Nikolaou, E. Agapaki, E. Nikoloudakis, K. Achilleos, K. Ladomenou, G. Charalambidis, E. Triantafyllou and A. G. Coutsolelos, *Chem. Commun.*, 2023, **59**, 11256–11259.
23 E. J. Pratt, E. I. Mancera-Andrade and K. L. Bicker, *ACS Omega*, 2022, **7**, 36663–36671.
24 E. Kaiser, R. L. Colescott, C. D. Bossinger and P. I. Cook, *Anal. Biochem.*, 1970, **34**, 595–598.
25 S. N. Baker and G. A. Baker, *Angew. Chem., Int. Ed.*, 2010, **49**, 6726–6744.
26 S.-T. Yang, L. Cao, P. G. Luo, F. Lu, X. Wang, H. Wang, M. J. Meziani, Y. Liu, G. Qi and Y.-P. Sun, *J. Am. Chem. Soc.*, 2009, **131**, 11308–11309.
27 S. L. D'Souza, B. Deshmukh, J. R. Bhamore, K. A. Rawat, N. Lenka and S. K. Kailasa, *RSC Adv.*, 2016, **6**, 12169–12179.
28 Z. Liang, L. Zeng, X. Cao, Q. Wang, X. Wang and R. Sun, *J. Mater. Chem. C*, 2014, **2**, 9760–9766.
29 E. Nikoloudakis, M. Pigiaki, M. N. Polychronaki, A. Margaritopoulou, G. Charalambidis, E. Serpetzoglou, A. Mitraki, P. A. Loukakos and A. G. Coutsolelos, *ACS Sustainable Chem. Eng.*, 2021, **9**, 7781–7791.
30 P. G. Luo, S. Sahu, S.-T. Yang, S. K. Sonkar, J. Wang, H. Wang, G. E. LeCroy, L. Cao and Y.-P. Sun, *J. Mater. Chem. B*, 2013, **1**, 2116–2127.
31 A. B. Bourlinos, A. Stassinopoulos, D. Anglos, R. Zboril, M. Karakassides and E. P. Giannelis, *Small*, 2008, **4**, 455–458.
32 S. Zhu, Q. Meng, L. Wang, J. Zhang, Y. Song, H. Jin, K. Zhang, H. Sun, H. Wang and B. Yang, *Angew. Chem., Int. Ed.*, 2013, **52**, 3953–3957.
33 T. E. Shubina, H. Marbach, K. Flechtner, A. Kretschmann, N. Jux, F. Buchner, H.-P. Steinrück, T. Clark and J. M. Gottfried, *J. Am. Chem. Soc.*, 2007, **129**, 9476–9483.
34 R. Zanoni, A. Aurora, F. Cattaruzza, F. Decker, P. Fastiggi, V. Menichetti, P. Tagliatesta, A. L. Capodilupo and A. Lembo, *Mater. Sci. Eng., C*, 2007, **27**, 1351–1354.
35 M. Tountas, A. Verykios, E. Polydorou, A. Kaltzoglou, A. Soultati, N. Balis, P. A. Angaridis, M. Papadakis, V. Nikolaou, F. Auras, L. C. Palilis, D. Tsikritzis, E. K. Evangelou, S. Gardelis, M. Koutsoureli, G. Papaioannou, I. D. Petsalakis, S. Kennou, D. Davazoglou, P. Argitis, P. Falaras, A. G. Coutsolelos and M. Vasilopoulou, *ACS Appl. Mater. Interfaces*, 2018, **10**, 20728–20739.
36 K. Flechtner, A. Kretschmann, L. R. Bradshaw, M.-M. Walz, H.-P. Steinrück and J. M. Gottfried, *J. Phys. Chem. C*, 2007, **111**, 5821–5824.
37 B. C. M. Martindale, E. Joliat, C. Bachmann, R. Alberto and E. Reisner, *Angew. Chem., Int. Ed.*, 2016, **55**, 9402–9406.
38 S. Schnidrig, C. Bachmann, P. Müller, N. Weder, B. Spingler, E. Joliat-Wick, M. Mosberger, J. Windisch, R. Alberto and B. Probst, *ChemSusChem*, 2017, **10**, 4570–4580.
39 F. Arcudi, V. Strauss, L. Đorđević, A. Cadranel, D. M. Guldi and M. Prato, *Angew. Chem., Int. Ed.*, 2017, **56**, 12097–12101.
40 F. D'Souza, S. Gadde, M. E. Zandler, K. Arkady, M. E. El-Khouly, M. Fujitsuka and O. Ito, *J. Phys. Chem. A*, 2002, **106**, 12393–12404.
41 P. M. Gharat, J. M. Chethodil, A. P. Srivastava, P. K. Praseetha, H. Pal and S. D. Choudhury, *Photochem. Photobiol. Sci.*, 2019, **18**, 110–119.
42 I. Sargin, G. Yanalak, G. Arslan and I. H. Patir, *Int. J. Hydrogen Energy*, 2019, **44**, 21781–21789.
43 A. Mehta, D. Pooja, A. Thakur and S. Basu, *New J. Chem.*, 2017, **41**, 4573–4581.
44 X. Xu, Z. Bao, G. Zhou, H. Zeng and J. Hu, *ACS Appl. Mater. Interfaces*, 2016, **8**, 14118–14124.
45 Y. J. Yuan, D. Chen, J. Zhong, L. X. Yang, J. J. Wang, Z. T. Yu and Z. G. Zou, *J. Phys. Chem. C*, 2017, **121**, 24452–24462.
46 C. Ménard-Moyon, C. Fabbro, M. Prato and A. Bianco, *Chem. – Eur. J.*, 2011, **17**, 3222–3227.
47 S. L. Pilicer and C. Wolf, *J. Org. Chem.*, 2020, **85**, 11560–11565.

